Theoretical Modelling for the Ground State Rotamerisation and Excited State Intramolecular Proton Transfer of 2-(2'-hydroxyphenyl)oxazole, 2-(2'-hydroxyphenyl)imidazole, 2-(2'-hydroxyphenyl)thiazole and Their Benzo Analogues

Pradipta Purkayastha[†] and Nitin Chattopadhyay*

Department of Chemistry, Jadavpur University, Calcutta - 700 032, India.
E-mail: pcnitin@yahoo.com
[†] Present address: Department of Chemistry, University of Pennsylvania, Philadelphia, PA 19104.

Abstract: Two series of compounds, one comprising of 2-(2'-hydroxyphenyl)benzoxazole (HBO), 2-(2'-hydroxyphenyl)benzimidazole (HBI), 2-(2'-hydroxyphenyl)benzothiazole (HBT), and the other of 2-(2'-hydroxyphenyl)oxazole (HPO), 2-(2'-hydroxyphenyl)imidazole (HPI) and 2-(2'-hydroxyphenyl)thiazole (HPT) are susceptible to ground state rotamerization as well as excited state intramolecular proton transfer (ESIPT) reactions. Some of these compounds show experimental evidence of the existence of two ground state conformers. Out of these two one undergoes ESIPT reaction leading to the formation of the tautomer. The two photophysical processes, in combination, result in the production of a number of fluorescence bands each one of which corresponding to a particular species. Semiempirical AM1-SCI calculations have been performed to rationalize the photophysical behaviour of the compounds. The calculations suggest that for the first series of compounds, two rotational isomers are present in the ground state of HBO and HBI while HBT has a single conformer under similar circumstances. For the molecules of the other series existence of rotamers depends very much on the polarity of the environment. The potential energy curves (PEC) for the ESIPT process in different electronic states of the molecules have been generated theoretically. The simulated PECs reveal that for all these systems the IPT reaction is unfavourable in the ground state but feasible, both kinetically and thermodynamically, in the S_1 as well as T_1 states.

Keywords: Rotamerization; excited state intramolecular proton transfer; oxazole, imidazole; thiazole; tautomer; AM1.

Introduction

Excited state intramolecular proton transfer (ESIPT) is complementary to the excited state intermolecular proton transfer (ESPT) in the subject of photoexcited state proton transfer reaction. The huge potential in the ESIPT process has provoked massive interest among the photophysicists and photochemists. Studies range from the choice of a variety of homo- and heterocyclic aromatic molecular systems to a wide variety of pure and mixed homogeneous and microheterogeneous solvents [1-11]. This phenomenon has widespread implications in photostabilizers [12], laser dyes [13] and also in the biological fields [14]. In organic bifunctional molecules, containing both the hydrogen atom donor and acceptor groups in close proximity, an intramolecular hydrogen bond is generally formed in the ground electronic state [15]. A distance of < 2 Å between the donor and the acceptor atom favours the migration of the proton to produce a phototautomer in the excited state [16]. The ESIPT process is extremely fast occurring within subpicosecond time scale that falls within the range of the period of low frequency vibrations. The Franck-Condon excited state of the molecule is very close to the intersection zone of the potential energy surfaces of the two prototropic species. Thus, upon excitation, the molecule passes to the potential well of the tautomeric species almost instantaneously and then relaxes vibrationally [17-21]. The tautomeric transformation barrier is very low; greater than the energies of the lowest frequency vibrations but similar to, or smaller than those of the stretching modes of the concerned compound skeleton. Analysis of the molecular geometry as a function of the reaction coordinate for the phototropic process shows that the proton transfer process takes place in the molecular plane [22].

The family of molecules in the azole category has been dealt with by several research groups in explaining the various aspects of excited state intramolecular proton transfer [21-30]. The early studies on 2-(2′-hydroxyphenyl)benzoxazole (HBO) and 2-(2′-hydroxyphenyl)benzothiazole (HBT) were done by Cohen and Flavian [31,32], who compared the behaviour of these compounds with N-nitrosalicylideneanilines in different solvents. Various experiments were performed by Elsaesser and Kaiser [33,34] on ESIPT of HBT in the picosecond time scale. Their visible and infrared spectroscopic data suggested that the potential energy surface of the transferred proton is anharmonic. The transient absorption kinetics of the keto-enol tautomerization of HBO and its derivatives in the triplet state displays the hydrogen-tunneling and the isotope effects in the process when the former molecules are coupled with their deutero derivatives [35]. The studies were further extended by Douhal *et al.* [36] to low temperature measurements using femtosecond spectroscopy. The time-resolved measurements indicate a short-lived initial Franck-Condon distribution that evolves into a distribution of vibrational levels which partly belong to the excited keto form of the molecule. They have also calculated the molecular geometry of the excited enol and keto forms using the MNDO methods [36]. Effect of rotamerism and hydrogen bonding on the ESIPT in HBO and HBI has also been studied using steady-state and time-resolved emission spectroscopy at various temperatures and by semi-empirical quantum mechanical methods like CNDO/SCI and AM1 [16,37].

Spectroscopic and theoretical studies have also been performed with compounds of the second series, *viz.*, 2-(2′-hydroxyphenyl)oxazole (HPO), 2-(2′-hydroxyphenyl)imidazole (HPI), 2-(2′-hydroxyphenyl)thiazole (HPT) [27,38]. Though reports are limited, the experimental observations with this group of compounds grossly run parallel to those for the compounds of the other group.

The overall photophysics of the compounds of the two series, comprised of the ground state rotamerization and ESIPT, follows a strict conformational requirement. Scheme 1 shows the structures of the three possible isomeric forms involved.
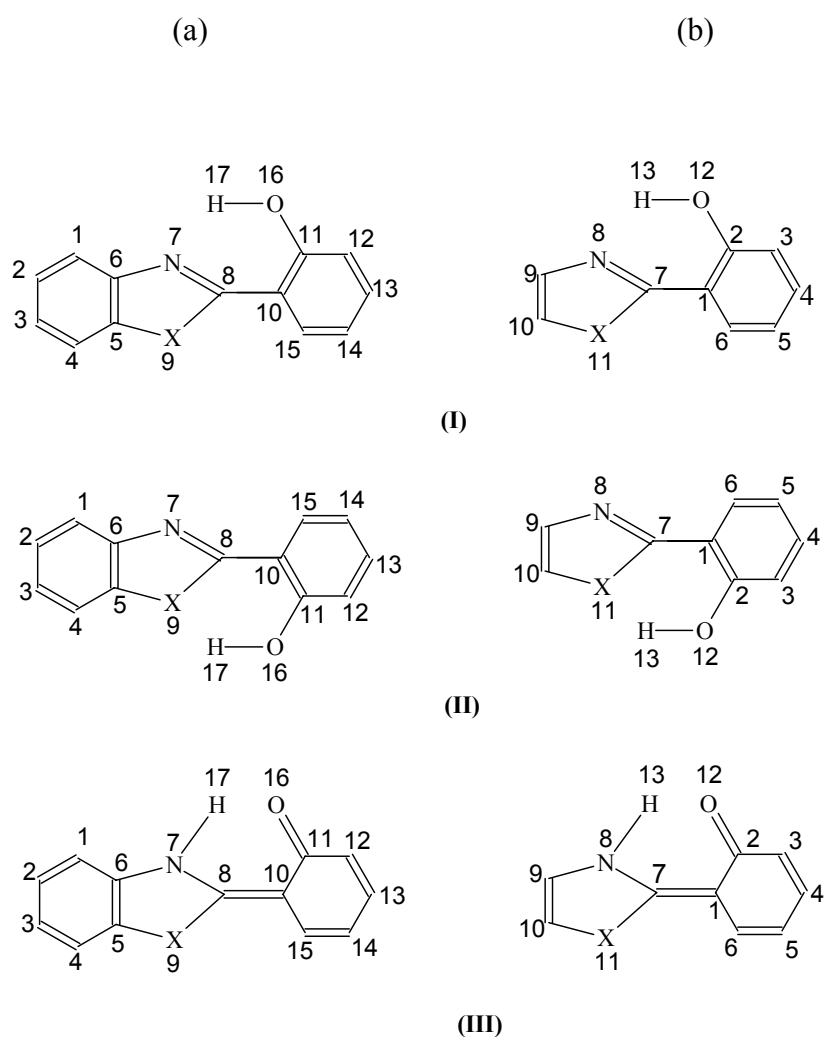
Scheme 1. The normal (I), rotamer (II) and tautomer (III) species of (a) HBO, HBI, HBT and (b) HPO, HPI and HPT. (X = -O-, -NH- and -S- for oxazole, imidazole and thiazole, respectively).

In principle, there may be two possible intramolecularly hydrogen bonded rotamers. However, experiments suggest that upon excitation only the normal form (**I** in scheme 1) undergoes ESIPT to give the corresponding tautomer resulting in an emission with a large stokes shift [39]. The rotamer (**II** in scheme 1) does not undergo ESIPT reaction and its short wavelength emission shows a mirror image relation with the corresponding absorption [16]. The excitation spectra of the rotamer and the tautomer emission show a large change in their relative intensities with a change in temperature. There is also a difference in the temporal behaviour of the fluorescence decay of the rotamer and the formation of the tautomer [18,39]. These evidences indicate that the electronic excitation of the species leads to the ESIPT product from only one of the two rotameric forms in selected solvents [23,25,27,28,33-35,37,39-50]. Mordzinski and Grellmann suggested that a thermally activated radiationless transition dominates the decay of the photoproduced keto form at room temperature, whereas, at lower temperature, fluorescence and intersystem crossing are the main deactivation processes [40]. The effects of hydrogen tunnelling and isotopic substitution on the keto-enol tautomerization in HBO were added investigations [35]. Apart from different homogeneous media, the photophysics of HBO has also been studied in microheterogeneous environments provided by the cyclodextrins [7,9].

Several theoretical works including *ab initio* [23,44], density functional theory [25,45] and semiempirical methods [49-52] have corroborated different aspects of the experimental findings in various ways. However, these theoretical studies are rather scattered. The theoretical description of the ESIPT trajectory and hence its thermodynamic and/or kinetic aspects have hardly been attempted in detail. Furthermore, there is still a lack of sufficient experimental data for the series HPO, HPI and HPT in terms of their photophysics. The success of the simple modelling in explaining the ground state rotamerization and excited state intramolecular photoprocesses for the two above mentioned series of compounds in our previous works [51,52] led us to make, for the general readers, a comprehensive theoretical study on the related aspects of the two series of compounds together in a common framework. The semi-empirical AM1-SCI method has been used for the calculations. The excitation, fluorescence and phosphorescence spectral positions for the corresponding molecules have been assigned from the different energy states in some selected solvents and compared with the available literature data. The feasibility of ESIPT reaction in the compounds has been corroborated from the simulated potential energy curves (PEC) for the intramolecular proton transfer (IPT) process.

Quantum Chemical Calculations

Although *ab initio* calculation is more reliable than the semi-empirical ones because there is no *apriori* approximation involved in the former, from the practical point of view this method can be applied only to small molecular systems. For larger molecules semi-empirical molecular orbital methods are better compromise as they are some orders of magnitude faster than the *ab initio* method

and give calculated results which agree with the experimental ones within acceptable limits [48-53]. The commercial package, HYPERCHEM 5.01 has been used for the present semi-empirical calculations [56]. The ground state (S_0) geometries of the molecules have been optimized using the AM1 method. Subsequently, AM1-SCI (singly excited configuration interaction) has been performed to get the ground state energy (E_g), dipole moments in the ground and excited states and the transition energies ($\Delta E_{i \to j}$) to different excited electronic states. For the CI calculations we have considered only the single electronic transitions between all the configurations (around 100 in number) within a predefined energy window (13-14 eV, depending on the molecular system) from the ground state. $\Delta E_{i \to j}$ corresponds to the excitation of an electron from the orbital ϕ_i (occupied in the ground state) to the orbital ϕ_j (unoccupied in the ground state). The total energy of the excited state (E_j) was then calculated as $E_j = E_g + \Delta E_{i \to j}$. The CI wavefunctions have been used to generate orbitals and one-electron density matrices, which were used, in turn, to calculate the dipole moments of the excited states of the molecular systems. The nature of the electronic transitions has been determined from the individual eigenvectors.

To find the relative stability of the different rotational conformers (rotamers), the torsional angle between the hydroxyphenyl plane and the heterocyclic plane has been preset to different values followed by a full optimization of all other geometrical parameters. With these optimized structures, the SCI was performed within the aforesaid energy window to get the energies and dipole moments corresponding to the ground (S_0) as well as different excited electronic states (S_1, T_1, etc.).

To study the intramolecular proton transfer (IPT) reaction, the potential energy curves (PEC) for the process have been generated. The distance between the dissociable hydrogen of the hydroxyl group and the nitrogen atom (to which the hydrogen gets attached when tautomer is formed) involved in the process has been considered as the reaction coordinate. The total procedure was repeated to get the energies and dipole moments of the species on the trajectory of the reaction in different electronic states. The PECs in the corresponding electronic states give the enthalpy of reaction (ΔH) and activation energy (E_{act}) for the IPT reaction of the fluorophores.

The solvent stabilization of the different states has been calculated from the solvation energies based on Onsager's theory [57]. Assuming that the solute molecule, having a dipole moment μ_i in the ith electronic state, to be fully solvated, the solvation energy is given by

$$\Delta E_{solv.} = \frac{2\mu_i^2(\varepsilon_r - 1)}{a^3(2\varepsilon_r + 1)}$$

where ε_r is the bulk relative permittivity of the solvent and a, the cavity radius. The maximum molecular length for the optimized geometry has been taken as the cavity diameter for the molecular systems (10.92, 10.94 and 11.14 Å for HBO, HBI, HBT and 8.50, 8.46 and 8.72 Å for HPO, HPI, HPT

respectively). It is pertinent to mention here that specific short range interactions like hydrogen bonding etc. have not been considered for the present work.

Results and Discussion

To establish the applicability and to ensure the reliability of the present method of calculation we have compared the structural data obtained from our semi-empirical AM1 calculation with those of the crystallographic ones reported in the literature. The crystallographic data are readily available for HBT [58] and 2-(3-methoxy-2-hydroxyphenyl)benzimidazole (MHBI) [59]. Table 1 compares the calculated parameters of the optimized ground state geometries with the crystallographic data for both the molecular systems [60]. Considering that the calculations are semiempirical (AM1), the agreement between the calculated data and the crystallographic ones are reasonably good.
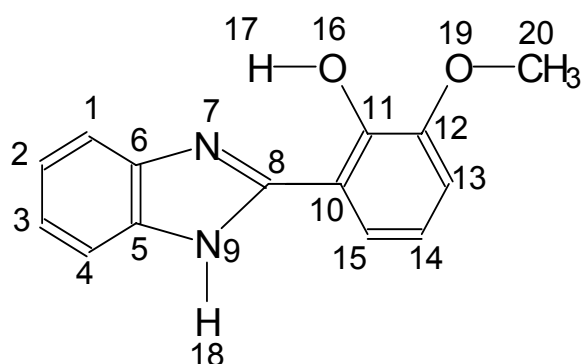
Scheme 2. Structure of MHBI.

Table 1. Comparison of the calculated ground state optimized geometric parameters of HBT and MHBI with the crystallographic data [bond length (Å) and angles (°)].

HBT[a]			MHBI[b]		
Molecular parameter	Calculated	Cryst. data[c]	Molecular parameter	Calculated	Cryst. data[d]
$O_{16}-C_{11}$	1.366	1.305	$O_{16}-C_{11}$	1.366	1.353
N_7-C_8	1.327	1.280	N_7-C_8	1.353	1.325
N_7-C_6	1.400	1.404	N_7-C_6	1.407	1.391
S_9-C_8	1.751	1.749	N_9-C_8	1.417	1.371
S_9-C_5	1.687	1.757	N_9-C_5	1.395	1.376
			$O_{19}-C_{12}$	1.380	1.377
			$O_{19}-C_{20}$	1.423	1.419
$C_8-N_7-C_6$	110.3	110.8	$C_8-N_7-C_6$	105.7	106.1
$C_8-S_9-C_5$	91.0	88.6	$C_8-N_9-C_5$	106.7	107.6
			$C_{12}-O_{19}-C_{20}$	115.9	117.1

[a] For the structure of HBT see Scheme 1 (form I). [b] For the structure of MHBI see Scheme 2.
[c] From ref. [58]. [d] From ref. [59].

Intramolecular rotation

Table 2 presents the various calculated geometric parameters of the different rotameric and prototropic species of HBO, HBI, HBT and HPO, HPI, HPT in different electronic states. The table reflects the stability of the normal form (I) over the rotamer (II) and the tautomer (III) in the ground state for all the compounds. The calculated energies, E (in eV) and dipole moments, μ (in debye), of the different species have also been calculated in different electronic states. The torsional angles (in degrees) and the interatomic distances (in Å) at the proton transfer site of the optimized isomers have also been presented in the table.

Figures 1-6 reflect the simulated energy profiles for the intramolecular rotation of the hydroxylphenyl moiety relative to the heterocyclic ring for the molecules of both the series in different electronic states to examine the existence of the different conformational isomers. The figures present the energy diagrams for the bare molecules along with their solvated species in ethanol.

Figures 1 and 2 demonstrate the existence of the normal (I) and rotameric (II) forms of HBO and HBI in the ground state which is supported by the experimental observations [16,37,39]. Nagaoka *et al.* [44] and Das *et al.* [16] also reported the existence of the two rotameric forms (I and II) of HBO in the ground state from their *ab initio* (STO-3G) and semiempirical (CNDO/SCI) calculations respectively. However, slight discrepancy has crept into the reported ground state geometry of the rotational isomers. Present calculations show that the monitored dihedral angles ($T_{7-8-10-11}$) for I and II of HBO are 0° and 150° respectively. Nagaoka *et al.* got them as 0° and 180° and Das *et al.* found the values to be 30° and 180° respectively. The corresponding angles for the similar ground state rotameric species (I and II) of HBI are calculated to be 40° and 140° which match with those calculated by Das *et al.* [16]. Figure 3 indicates the existence of only one stable form of HBT in the ground state, the normal (I) one. Calculation shows insignificant energy barrier for the interconversion between the

Table 2. Equilibrium parameters of different photoisomers of HBO, HBI, HBT and HPO, HPI, HPT in different electronic states. R_{7-17} represents the interatomic distance between the two atoms for the first series and R_{8-13} represents it for the other series referred to by the numbers (see Scheme 1). $T_{7-8-10-11}$ is the torsional angle developed by the atoms of the first series and $T_{2-1-7-8}$ is that developed by those of the second series.

Molecules	Parameters	Normal (**I**)	Rotamer (**II**)	Tautomer (**III**)
HBO	$E\,(S_0)$	-126.4425	-126.4369	-126.0482
	$\mu\,(S_0)$	1.77	0.80	4.26
	R_{7-17}	2.17	3.70	0.996
	$T_{7-8-10-11}$	0	150	0
	$E\,(S_1)$	-122.9232	-122.8528	-123.0303
	$\mu\,(S_1)$	1.15	1.33	3.08
	$T_{7-8-10-11}$	0	180	0
	$E\,(T_1)$	-123.9292	-123.8853	-124.4109
	$\mu\,(T_1)$	1.84	1.19	2.22
	$T_{7-8-10-11}$	0	180	0

Table 2. Continued.

Molecules	Parameters	Normal (**I**)	Rotamer (**II**)	Tautomer (**III**)
HBI	$E(S_0)$	-129.5468	-129.5230	-129.1756
	$\mu(S_0)$	3.36	1.67	5.49
	R_{7-17}	2.29	3.67	0.998
	$T_{7-8-10-11}$	40	140	0
	$E(S_1)$	-126.0484	-125.9378	-126.2733
	$\mu(S_1)$	2.65	1.97	4.00
	$T_{7-8-10-11}$	0	160	0
	$E(T_1)$	-126.9800	-126.8966	-127.4739
	$\mu(T_1)$	3.07	1.19	3.43
	$T_{7-8-10-11}$	0	160	0
HBT	$E(S_0)$	-125.8044	—	-125.4224
	$\mu(S_0)$	2.11	—	4.03
	R_{7-17}	2.16	—	1.00
	$T_{7-8-10-11}$	0	—	0
	$E(S_1)$	-122.4303	—	-122.7835
	$\mu(S_1)$	2.00	—	0.85
	$T_{7-8-10-11}$	0	—	0
	$E(T_1)$	-123.3868	—	-124.0442
	$\mu(T_1)$	1.80	—	2.72
	$T_{7-8-10-11}$	0	—	0
HPO	$E(S_0)$	-93.0181	-93.0060	-92.5105
	$\mu(S_0)$	2.08	0.87	4.58
	R_{8-13}	2.18	3.69	0.997
	$T_{2-1-7-8}$	0	150	0
	$E(S_1)$	-89.4435	-89.3764	-89.4581
	$\mu(S_1)$	1.01	1.74	3.96
	$T_{2-1-7-8}$	0	170	0
	$E(T_1)$	-90.9033	-90.8851	-91.0296
	$\mu(T_1)$	1.84	0.80	2.42
	$T_{2-1-7-8}$	0	180	0
HPI	$E(S_0)$	-96.0248	-96.0043	-95.0158
	$\mu(S_0)$	3.88	1.97	6.33
	R_{8-13}	2.33	3.69	1.00
	$T_{2-1-7-8}$	40	140	0
	$E(S_1)$	-92.4601	-92.2281	-92.5831
	$\mu(S_1)$	2.91	2.57	5.36
	$T_{2-1-7-8}$	0	140	0
	$E(T_1)$	-93.7735	-93.7452	-93.9393
	$\mu(T_1)$	3.04	1.83	4.15
	$T_{2-1-7-8}$	0	180	0
HPT	$E(S_0)$	-92.2318	—	-91.7456
	$\mu(S_0)$	2.54	—	4.00
	R_{8-13}	2.14	—	1.00
	$T_{2-1-7-8}$	10	—	0
	$E(S_1)$	-88.9889	—	-89.3397
	$\mu(S_1)$	1.62	—	1.15
	$T_{2-1-7-8}$	0	—	0
	$E(T_1)$	-90.2039	—	-90.4719
	$\mu(T_1)$	1.83	—	2.44
	$T_{2-1-7-8}$	0	—	0

Figure 1. Plot of total molecular energy as a function of torsional angle (7-8-10-11) in S_0, S_1 and T_1 states of HBO (i, isolated; s, solvated in ethanol).
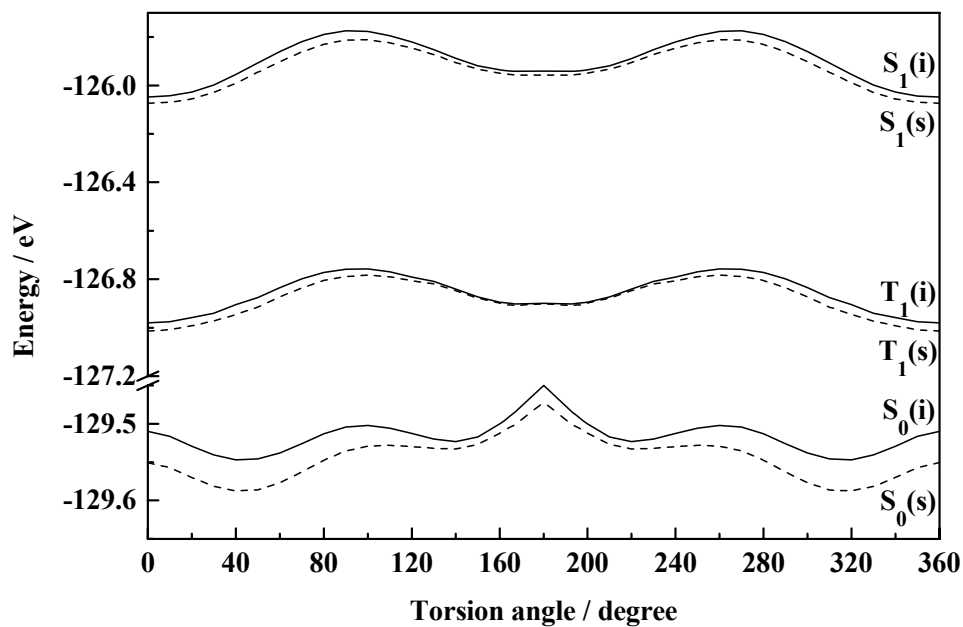
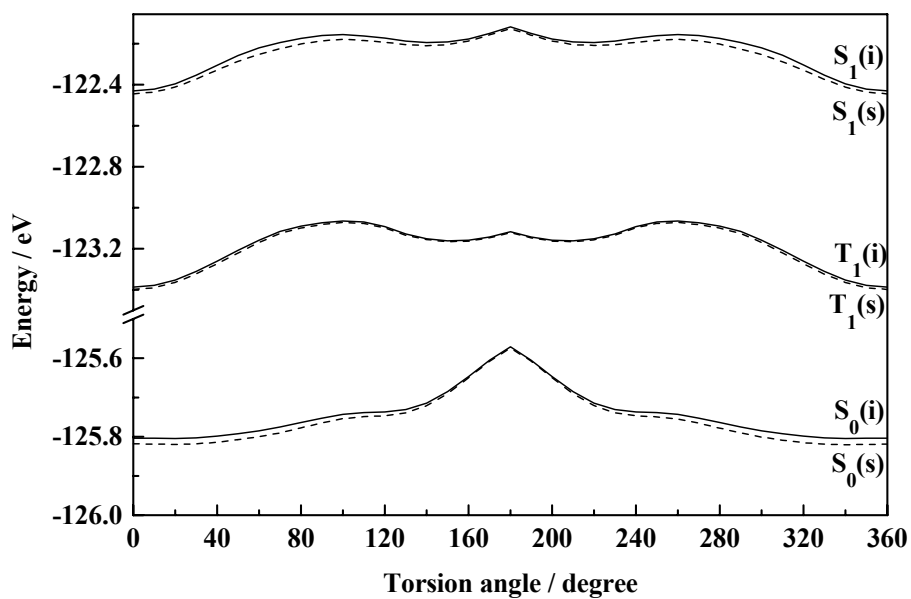**Figure 2.** Plot of total molecular energy as a function of torsional angle (7-8-10-11) in S_0, S_1 and T_1 states of HBI (i, isolated; s, solvated in ethanol).
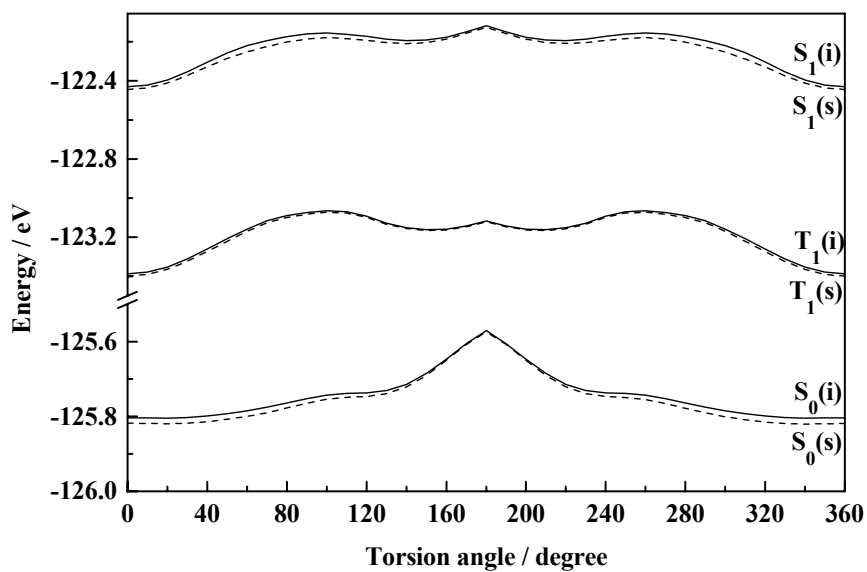
Figure 3. Plot of total molecular energy as a function of torsional angle (7-8-10-11) in S_0, S_1 and T_1 states of HBT (i, isolated; s, solvated in ethanol).

Figure 4. Plot of total molecular energy as a function of torsional angle (2-1-7-8) in S_0, S_1 and T_1 states of HPO (i, isolated; s, solvated in ethanol).

Figure 5. Plot of total molecular energy as a function of torsional angle (2-1-7-8) in S_0, S_1 and T_1 states of HPI (i, isolated; s, solvated in ethanol).

Figure 6. Plot of total molecular energy as a function of torsional angle (2-1-7-8) in S_0, S_1 and T_1 states of HPT (i, isolated; s, solvated in ethanol).
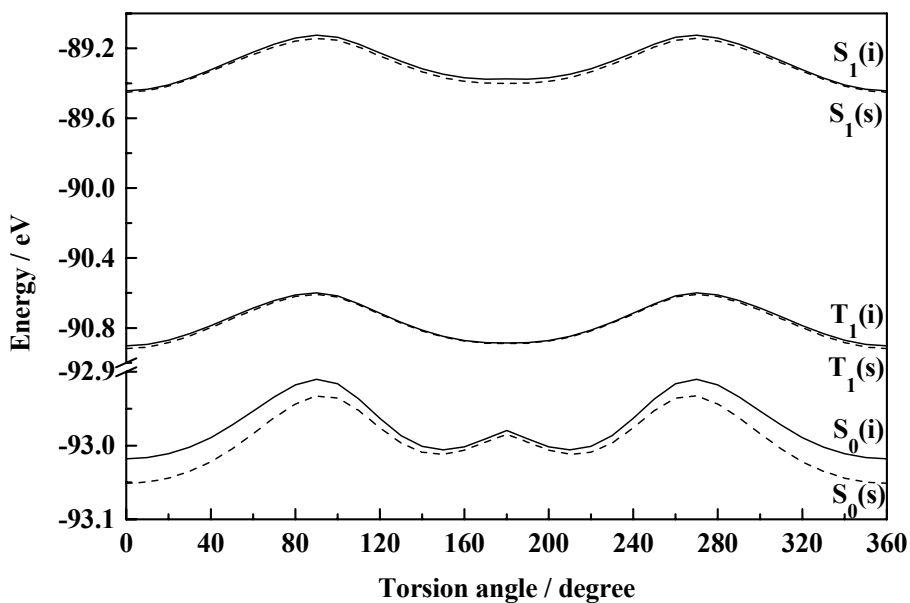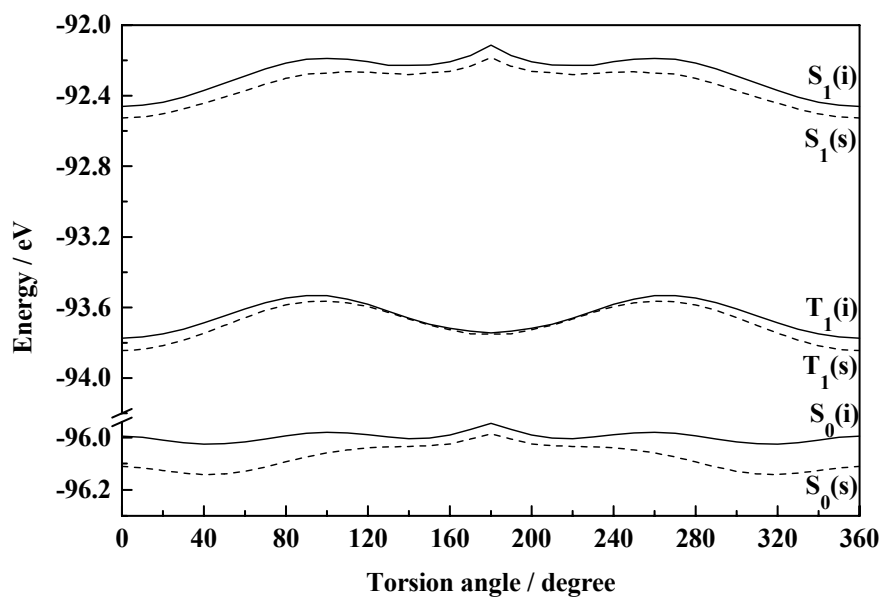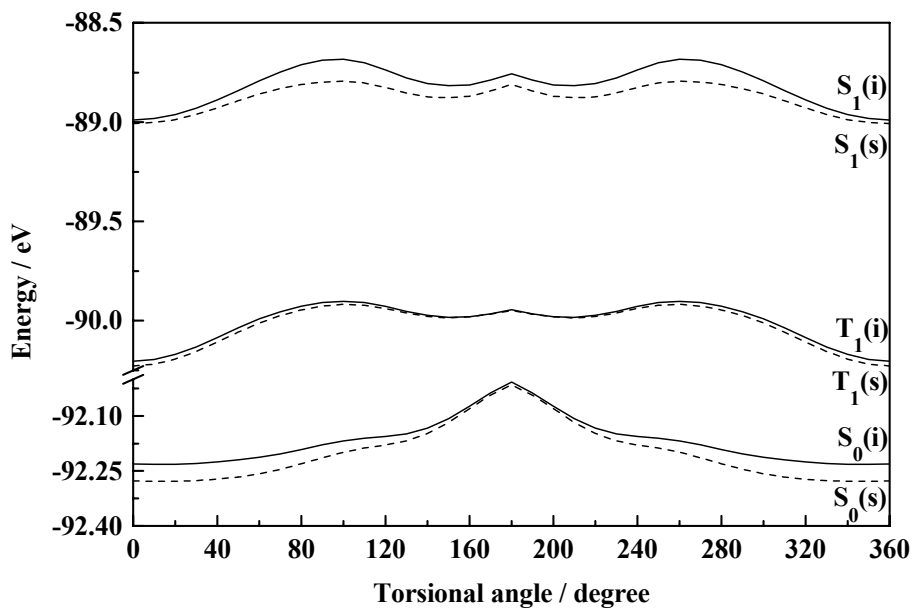
normal and rotameric forms and thus rules out the independent existence of the rotamer. The instability of the rotamer of HBT has been supported by Nagaoka *et al.* [44] from their *ab initio* calculations. The differential behaviour of HBT compared to that of HBO and HBI may be incurred due to the low electronegativity and the bulkier size of the sulfur atom [44]. The energy of activation for the interconversion of I to II has been calculated to be 0.101 eV and 0.045 eV for HBO and HBI respectively in the isolated conditions which are calculated to be 0.113 eV and 0.054 eV in ethanol solution. The barrier heights for the reverse transformation for the said molecules are 0.096 eV and 0.021 eV in isolated condition and 0.099 eV and 0.005 eV in ethanol solution respectively. The low energy barriers make a clear suggestion for the existence of the rotameric forms I and II in equilibrium. There is practically no energy barrier for II $\rightarrow$ I transformation in the case of HBT resulting in the nonexistence of form II of this system. The calculations, thus, support the existence of two isomers (the normal (I) and the rotamer (II)) of HBO and HBI and only the normal (I) species of HBT in the ground state. Tables 3, 4 and 5 represent the calculated energy values of S_0, S_1 and T_1 states of the different possible isomers (I, II and III) of HBO, HBI and HBT respectively in isolated and solvated conditions.

Table 3. Calculated S_0, S_1 and T_1 energies (eV) of the normal (I), rotamer (II) and tautomer (III) of HBO in isolated and solvated conditions (Onsager's cavity radius, $a = 5.46$ Å).

Medium / Solvent	Relative permittivity (ε_r)	Species	E (S_0)	E (S_1)	E (T_1)
vacuum	—	I	-126.4425	-122.9232	-123.9292
		II	-126.4369	-122.8528	-123.8853
		III	-126.0482	-123.0303	-124.4109
cyclohexane	2.0	I	-126.4474	-122.9253	-123.9345
		II	-126.4379	-122.8553	-123.8871
		III	-126.0766	-123.0450	-124.4185
p-dioxane	2.2	I	-126.4478	-122.9255	-123.9350
		II	-126.4380	-122.8553	-123.8876
		III	-126.0793	-123.0450	-124.4193
ethanol	24.3	I	-126.4538	-122.9280	-123.9415
		II	-126.4392	-122.8586	-123.8895
		III	-126.1140	-123.0645	-124.4287
acetonitrile	38	I	-126.4540	-122.9281	-123.9418
		II	-126.4393	-122.8588	-123.8896
		III	-126.1155	-123.0653	-124.4291
water	80	I	-126.4543	-122.9282	-123.9421
		II	-126.4393	-122.8589	-123.8897
		III	-126.1169	-123.0660	-124.4295

Table 4. Calculated S_0, S_1 and T_1 energies (eV) of the normal (I), rotamer (II) and tautomer (III) of HBI in isolated and solvated conditions (Onsager's cavity radius, $a = 5.47$ Å).

Medium / Solvent	Relative permittivity (ε_r)	Species	E (S_0)	E (S_1)	E (T_1)
vacuum	—	I	-129.5468	-126.0484	-126.9800
		II	-129.5230	-125.9378	-126.8966
		III	-129.1756	-126.2733	-127.4739
cyclohexane	2.0	I	-129.5641	-126.0592	-126.9944
		II	-129.5273	-125.9438	-126.8988
		III	-129.2220	-126.2980	-127.4919
p-dioxane	2.2	I	-129.5661	-126.0604	-126.9960
		II	-129.5278	-125.9445	-126.8991
		III	-129.2271	-126.3007	-127.4939
ethanol	24.3	I	-129.5875	-126.0738	-127.0139
		II	-129.5330	-125.9518	-126.9018
		III	-129.2845	-126.3312	-127.5163
acetonitrile	38	I	-129.5885	-126.0744	-127.0147
		II	-129.5333	-125.9522	-126.9019
		III	-129.2870	-126.3325	-127.5173
water	80	I	-129.5896	-126.0751	-127.0156
		II	-129.5336	-125.9525	-126.9020
		III	-129.2901	-126.3341	-127.5185

Table 5. Calculated S_0, S_1 and T_1 energies (eV) of the normal (I) and tautomer (III) of HBT in isolated and solvated conditions (Onsager's cavity radius, $a = 5.57$ Å)

Medium / Solvent	Relative permittivity (ε_r)	Species	E (S_0)	E (S_1)	E (T_1)
vacuum	—	I	-125.8044	-122.4303	-123.3868
		III	-125.4224	-122.7835	-124.0442
cyclohexane	2.0	I	-125.8110	-122.4362	-123.3916
		III	-125.4462	-122.7845	-124.0551
p-dioxane	2.2	I	-125.8116	-122.4368	-123.3920
		III	-125.4486	-122.7846	-124.0561
ethanol	24.3	I	-125.8196	-122.4440	-123.3978
		III	-125.4777	-122.7859	-124.0694
acetonitrile	38	I	-125.8199	-122.4443	-123.3981
		III	-125.4790	-122.7860	-124.0699
water	80	I	-125.8203	-122.4446	-123.3983
		III	-125.4802	-122.7860	-124.0705

The fact that the rotational behaviours of HPO, HPI and HPT are grossly similar to those of the corresponding benzo analogues is obvious from figures 1-6. Figure 4 demonstrates the existence of both normal (I) and the rotameric (II) forms for HPO in the ground state. The calculated values of the dihedral angles for the stable normal and rotameric forms in the ground state are found to be 0° and 150° respectively which resemble with those found for HBO through similar calculations. The intrinsic steric effect due to the lone electron pair on the oxygen atom in the heterocyclic ring and its effective size is probably responsible for the deviation of the torsional angle from 180°. It is thus, suggested that HPO and HBO have similar geometric arrangements. A comparison of the difference in the energies of the S_0 and S_1 states for HPO and HBO points to a red-shift of the observed absorption band in HBO relative to that in HPO and is ascribed to the extension of the conjugated system [27]. The rotamers (II) for both the compounds are less stable than the corresponding normal forms (I). The activation energy for the rotameric transformation I → II for HPO is about 0.108 eV in vacuum while that for HBO was calculated to be 0.101 eV. For the reverse transformation II → I the same has a magnitude of 0.105 eV and 0.096 eV for the two compounds respectively. The low energy barriers suggest that the species I and II remain in equilibrium at ambient temperature.

The existence of the normal (I) as well as the rotamer (II) of HPI in the ground state is suggested from figure 5. In low polarity solvents like cyclohexane and 1,4-dioxane both the species coexist. However, in more polar solvents, like ethanol, acetonitrile and water, the barrier for the stabilization of the two rotational isomers hardly exists. Although a near stability zone can be achieved as shown in the figure, but the distinct stability of both the species becomes a question in solvents of higher polarity. This leads to the nonexistence of the rotamer (II) of HPI in polar solvents in contrast to the situation for HBI where both the conformers exist in solvents of all polarity, the barrier for the interconversion, of course, decreases in polar solvents. The additional steric factor developed due to the presence of the 'N−H' group in HPI or HBI compared to '−O−' in HPO or HBO probably restricts the formation of the rotamer. The activation energies for the interconversion of I → II in HPI and HBI are found to be same (0.045 eV) in vacuum and those for the reverse process, i.e., II → I are 0.024 eV and 0.021 eV respectively. The dihedral angles corresponding to the normal (I) and the rotamer (II) of HPI and HBI are calculated to be 40° and 140° respectively.

Figure 6 demonstrates a considerable difference in the rotamerization characteristics of HPT in comparison with the other two members in the series. The rotamer (II) gets stabilization in neither isolated nor solvated conditions. The recent experimental study of Le Gourriérec *et al.* [27] rules out the existence of II and corroborates our proposition. The non-existence of the rotamer of HPT has been rationalized from a greater single bond character of the bond joining the phenol and the azole rings and thus allowing for more twisting vibrations whereby the rotamer is unable to get any well-defined stability. HBT and HPT behave similarly in this respect [44]. Tables 6, 7 and 8 report the calculated parameters for HPO, HPI and HPT respectively.

Table 6. Calculated S_0, S_1 and T_1 energies (eV) of the normal (I), rotamer (II) and tautomer (III) of HPO in isolated and solvated conditions (Onsager's cavity radius, $a = 4.25$ Å).

Medium / Solvent	Relative permittivity (ε_r)	Species	E (S_0)	E (S_1)	E (T_1)
vacuum	—	I	-93.0181	-89.4435	-90.9033
		II	-93.0060	-89.3764	-90.8851
		III	-92.5105	-89.4581	-91.0296
cyclohexane	2.0	I	-93.0322	-89.4467	-90.9099
		II	-93.0085	-89.3784	-90.8867
		III	-92.5790	-89.5094	-91.0487
p-dioxane	2.2	I	-93.0338	-89.4471	-90.9106
		II	-93.0088	-89.3855	-90.8869
		III	-92.5866	-89.5151	-91.0508
ethanol	24.3	I	-93.0511	-89.4512	-90.9188
		II	-93.0119	-89.3966	-91.0322
		III	-92.6713	-89.5786	-91.0744
acetonitrile	38	I	-93.0519	-89.4514	-90.9191
		II	-93.0120	-89.3970	-91.0336
		III	-92.6750	-89.5814	-91.0755
water	80	I	-93.0527	-89.4516	-90.9194
		II	-93.0121	-89.4006	-91.0358
		III	-92.6785	-89.5840	-91.0764

Table 7. Calculated S_0, S_1 and T_1 energies (eV) of the normal (I), rotamer (II) and tautomer (III) of HPI in isolated and solvated conditions (Onsager's cavity radius, $a = 4.23$ Å).

Medium / Solvent	Relative permittivity (ε_r)	Species	E (S_0)	E (S_1)	E (T_1)
vacuum	—	I	-96.0248	-92.4601	-93.7735
		II	-96.0043	-92.2281	-93.7452
		III	-95.0158	-92.5831	-93.9393
cyclohexane	2.0	I	-96.0748	-92.4882	-93.8041
		II	-96.0171	-92.2500	-93.7563
		III	-95.1484	-92.6783	-93.9963
p-dioxane	2.2	I	-96.0803	-92.4913	-93.8075
		II	-96.0186	-92.2524	-93.7575
		III	-95.1615	-92.6888	-94.0026
ethanol	24.3	I	-96.1418	-92.526	-93.8454
		II	-96.0344	-92.2795	-93.7713
		III	-95.3273	-92.8066	-94.0731
acetonitrile	38	I	-96.1443	-92.5275	-93.8471
		II	-96.0351	-92.2807	-93.7719
		III	-95.3344	-92.8117	-94.0762
water	80	I	-96.1470	-92.5290	-93.8487
		II	-96.0358	-92.2818	-93.7724
		III	-95.3412	-92.8166	-94.0790

Table 8. Calculated S_0, S_1 and T_1 energies (eV) of the normal (I), rotamer (II) and tautomer (III) of HPT in isolated and solvated conditions (Onsager's cavity radius, a = 4.36 Å).

Medium / Solvent	Relative permittivity (ε_r)	Species	E (S_0)	E (S_1)	E (T_1)
vacuum	—	I	-92.2318	-88.9889	-90.2039
		III	-91.7456	-89.3397	-90.4719
cyclohexane	2.0	I	-92.2516	-88.9967	-90.2138
		III	-91.7934	-89.3436	-90.4897
p-dioxane	2.2	I	-92.2537	-88.9976	-90.215
		III	-91.7987	-89.3441	-90.4916
ethanol	24.3	I	-92.2781	-89.0073	-90.2274
		III	-91.8578	-89.3490	-90.5136
acetonitrile	38	I	-92.2791	-89.0077	-90.2279
		III	-91.8604	-89.3492	-90.5146
water	80	I	-92.2801	-89.0081	-90.2284
		III	-91.8628	-89.3494	-90.5155

Assignment of the electronic spectra

The excitation, fluorescence and phosphorescence spectra of HBO, HBI, HBT and HPO, HPI, HPT in some common solvents differing in polarity have been calculated and discussed in this section. In pure and homogeneous solvents the solvation dynamics is faster than the fluorescence decay rate [61,62]. This leads the probe molecule to get solvated before it fluoresces. Correspondence between the fluorescence and the transition from the solvated S_1 state to the corresponding Franck-Condon S_0 state is, therefore, justified. Similar correlation is also viable for the excitation spectra with the transition between the solvated S_0 state and the Franck-Condon S_1 state. A crude assignment of the phosphorescence emission of the compounds, which obviously gets modified in solid matrix, has been made by calculating the transition energies from the solvated T_1 state to the corresponding Franck-Condon S_0 state. The assignments for the excitation, fluorescence and phosphorescence spectra of HBO, HBI and HBT fluorophores are presented in Tables 9, 10 and 11 respectively.

Similar assignments have been made for HPO, HPI and HPT and demonstrated in Tables 12, 13 and 14 respectively. It is pertinent to mention here that the positions of the experimental absorption bands are always at a little higher energy compared to the calculated absorption positions. This is because the calculated spectra represent the 0-0 transition only between the S_0 and S_1 states, while the experiments give rise to absorption bands with broad maxima leading to the transition to the upper vibrational levels of S_1 as well. From the proximity of the spectral data and our calculated transitions, we ascribe that the S_1 and T_1 states effective for the ESIPT process are both of $\pi\pi^*$ nature. This is consistent with the literature reports [16,25,27,33,50].

Table 9. Assignment of excitation, fluorescence and phosphorescence spectra of HBO in different solvents in terms of calculated energies (eV). Numbers within parentheses refer to the references corresponding to the experimental data. (n.a. indicates non-availability of data).

Solvent	Species	Excitation		Fluorescence		Phosphorescence	
		Calc.	Expt (ref)	Calc.	Expt (ref)	Calc.	Expt (ref)
cyclohexane	I	3.52	3.71 (39)	3.52	n.a.	2.51	n.a.
	II	3.59	3.88 (39)	3.58	3.40 (39)	2.55	n.a.
	III	—	—	3.00	2.60 (39)	1.63	n.a.
p-dioxane	I	3.52	n.a.	3.52	n.a.	2.51	n.a.
	II	3.59	n.a.	3.58	n.a.	2.55	n.a.
	III	—	—	2.98	n.a.	1.63	n.a.
ethanol	I	3.53	3.77 (39)	3.51	n.a.	2.50	2.30 (8)
	II	3.59	3.94 (39)	3.58	3.40 (39)	2.55	2.80 (8)
	III	—	—	2.98	2.64 (39)	1.62	n.a.
acetonitrile	I	3.53	3.77 (39)	3.51	n.a.	2.50	n.a.
	II	3.59	3.94 (39)	3.58	3.45 (39)	2.55	n.a.
	III	—	—	2.98	2.62 (39)	1.62	n.a.
water	I	3.53	3.77 (9)	3.51	n.a.	2.50	n.a.
	II	3.59	3.94 (9)	3.58	3.45 (9)	2.55	n.a.
	III	—	—	2.98	2.59 (9)	1.62	n.a.

Table 10. Assignment of excitation, fluorescence and phosphorescence spectra of HBI in different solvents in terms of calculated energies (eV). Numbers within parentheses refer to the references corresponding to the experimental data. (n.a. indicates non-availability of data).

Solvent	Species	Excitation		Fluorescence		Phosphorescence	
		Calc.	Expt (ref)	Calc.	Expt (ref)	Calc.	Expt (ref)
cyclohexane	I	3.52	3.70 (53)	3.49	n.a.	2.55	n.a.
	II	3.59	3.88 (53)	3.58	n.a.	2.49	n.a.
	III	---	---	2.88	n.a.	1.68	n.a.
p-dioxane	I	3.52	n.a.	3.49	n.a.	2.55	n.a.
	II	3.59	n.a.	3.58	3.55 (16)	2.49	n.a.
	III	---	---	2.87	2.64 (16)	1.68	n.a.
ethanol	I	3.54	3.75 (37)	3.47	n.a.	2.53	n.a.
	II	3.60	3.80 (37)	3.57	3.60 (37)	2.47	n.a.
	III	---	---	2.84	3.10 (37)	1.66	n.a.
acetonitrile	I	3.54	n.a.	3.47	n.a.	2.53	n.a.
	II	3.60	n.a.	3.57	n.a.	2.47	n.a.
	III	---	---	2.84	n.a.	1.66	n.a.
water	I	3.54	n.a.	3.47	n.a.	2.53	n.a.
	II	3.60	n.a.	3.57	3.55 (16)	2.47	n.a.
	III	---	---	2.84	2.86 (16)	1.66	n.a.

Table 11. Assignment of excitation, fluorescence and phosphorescence spectra of HBT in different solvents in terms of calculated energies (eV). Numbers within parentheses refer to the references corresponding to the experimental data. (n.a. indicates non-availability of data).

Solvent	Species	Excitation		Fluorescence		Phosphorescence	
		Calc.	Expt (ref)	Calc.	Expt (ref)	Calc.	Expt (ref)
cyclohexane	I	3.38	n.a.	3.37	n.a.	2.41	n.a.
	III	—	—	2.64	n.a.	1.37	n.a.
p-dioxane	I	3.38	n.a.	3.37	n.a.	2.41	n.a.
	III	—	—	2.64	n.a.	1.37	n.a.
ethanol	I	3.39	3.77 (41)	3.36	3.36 (41)	2.41	n.a.
	III	—	—	2.64	2.70 (41)	1.35	n.a.
acetonitrile	I	3.39	n.a.	3.36	n.a.	2.41	n.a.
	III	—	—	2.64	n.a.	1.35	n.a.
water	I	3.39	n.a.	3.36	n.a.	2.41	n.a.
	III	—	—	2.64	n.a.	1.35	n.a.

Table 12. Assignment of excitation, fluorescence and phosphorescence spectra of HPO in different solvents in terms of calculated energies (eV). Numbers within parentheses refer to the references corresponding to the experimental data. (n.a. indicates non-availability of data).

Solvent	Species	Excitation		Fluorescence		Phosphorescence	
		Calc.	Expt.*	Calc.	Expt.*	Calc.	Expt.*
cyclohexane	I	3.81	3.88	3.57	n.a.	2.11	n.a
	II	3.87	4.00	3.60	3.66	2.09	n.a.
	III	—	—	2.99	2.60	1.46	n.a.
p-dioxane	I	3.82	n.a.	3.57	n.a.	2.11	n.a.
	II	3.87	n.a.	3.60	n.a.	2.09	n.a.
	III	—	—	2.99	n.a.	1.46	n.a.
ethanol	I	3.83	3.93	3.57	n.a.	2.10	2.30 (63)
	II	3.87	4.06	3.59	3.60	2.09	2.80 (63)
	III	—	—	2.93	2.70	1.44	n.a.
acetonitrile	I	3.83	3.96	3.57	n.a.	2.10	n.a.
	II	3.87	4.06	3.59	3.60	2.09	n.a.
	III	—	—	2.93	2.70	1.43	n.a.
water	I	3.83	3.98	3.57	n.a.	2.10	n.a.
	II	3.87	4.10	3.59	3.55	2.09	n.a.
	III	—	—	2.93	2.79	1.43	n.a.

*The experimental values are taken from reference number [27] if not otherwise mentioned.

Table 13. Assignment of excitation, fluorescence and phosphorescence spectra of HPI in different solvents in terms of calculated energies (eV). Numbers within parentheses refer to the references corresponding to the experimental data. (n.a. indicates non-availability of data).

Solvent	Species	Excitation		Fluorescence		Phosphorescence	
		Calc.	Expt.	Calc.	Expt.	Calc.	Expt.
cyclohexane	I	3.96	3.88	3.51	n.a.	2.19	n.a
	II	3.87	4.00	3.75	n.a.	2.19	n.a.
	III	—	—	2.83	n.a.	1.51	n.a.
p-dioxane	I	3.97	n.a.	3.50	n.a.	2.19	n.a.
	II	3.87	n.a.	3.75	n.a.	2.19	n.a.
	III	—	—	2.82	n.a.	1.51	n.a.
ethanol	I	4.03	n.a.	3.47	n.a.	2.15	n.a.
	II	3.88	—	—	—	—	—
	III	—	—	2.70	n.a.	1.43	n.a.
acetonitrile	I	4.03	n.a.	3.47	n.a.	2.15	n.a.
	II	3.89	—	—	—	—	—
	III	—	—	2.70	n.a.	1.43	n.a.
water	I	4.03	n.a.	3.46	n.a.	2.15	n.a.
	II	3.89	—	—	—	—	—
	III	—	—	2.69	n.a.	1.43	n.a.

Table 14. Assignment of excitation, fluorescence and phosphorescence spectra of HPT in different solvents in terms of calculated energies (eV). Numbers within parentheses refer to the references corresponding to the experimental data. (n.a. indicates non-availability of data).

Solvent	Species	Excitation		Fluorescence		Phosphorescence	
		Calc.	Expt.*	Calc.	Expt.*	Calc.	Expt.*
cyclohexane	I	3.45	3.65	3.23	n.a.	2.02	n.a
	III	—	—	2.40	2.37	1.26	n.a.
p-dioxane	I	3.45	n.a.	3.23	n.a.	2.02	n.a.
	III	—	—	2.40	n.a.	1.25	n.a.
ethanol	I	3.47	3.72	3.22	n.a.	2.00	n.a.
	III	—	—	2.40	2.46	1.23	n.a.
acetonitrile	I	3.47	3.72	3.22	n.a.	2.00	n.a.
	III	—	—	2.40	2.46	1.23	n.a.
water	I	3.48	n.a.	3.22	n.a.	2.00	n.a.
	III	—	—	2.40	2.48	1.23	n.a.

*Since the experimental values for HPT system are not available, the data in the table refer to the spectral positions for 2-(2′-hydroxyphenyl)-4-methylthiazole and they have been taken from reference [27].

Intramolecular proton transfer

The potential energy curves (PEC) for the intramolecular proton transfer (IPT) process of the probes have been generated in S_0, S_1 and T_1 states, considering the distance between the migrating hydrogen atom and the relevant heteroatom to which the hydrogen is joined after proton transfer. Figures 7-12 represent the simulated PECs for the IPT process of the fluorophores HBO, HBI, HBT, HPO, HPI and HPT respectively in the three electronic states in isolated as well as in ethanolic solutions.
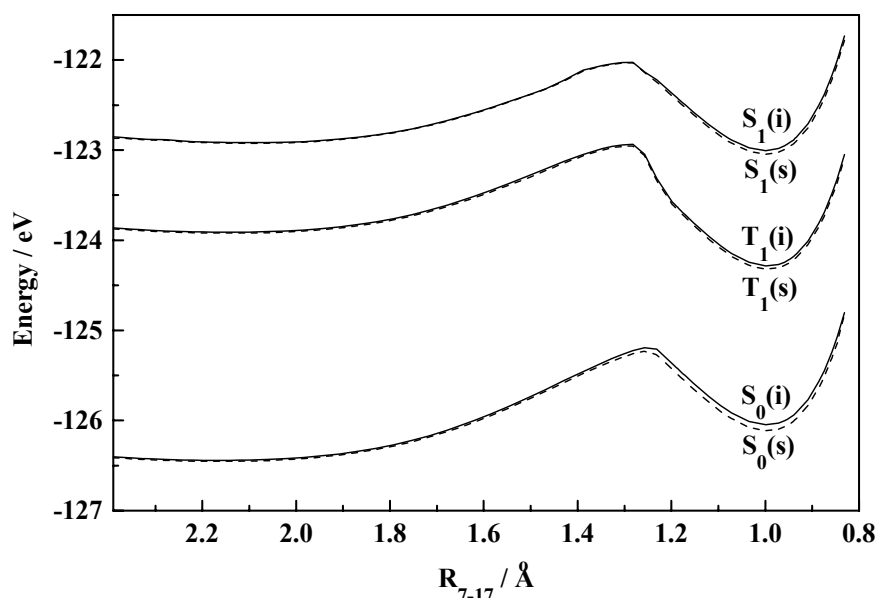
Figure 7. Simulated PECs for IPT process of HBO in S_0, S_1 and T_1 states (i, isolated; s, solvated in ethanol).
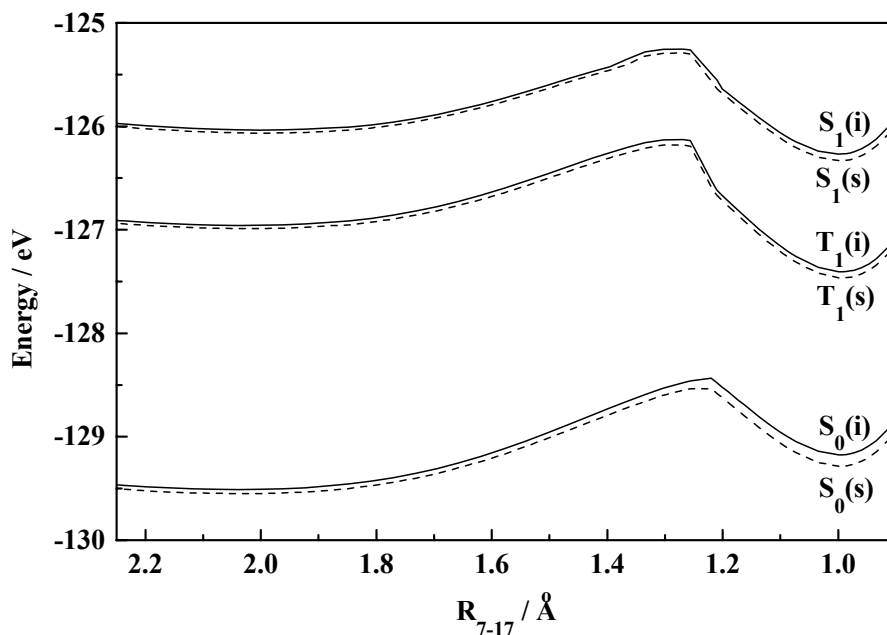
Figure 8. Simulated PECs for IPT process of HBI in S_0, S_1 and T_1 states (i, isolated; s, solvated in ethanol).
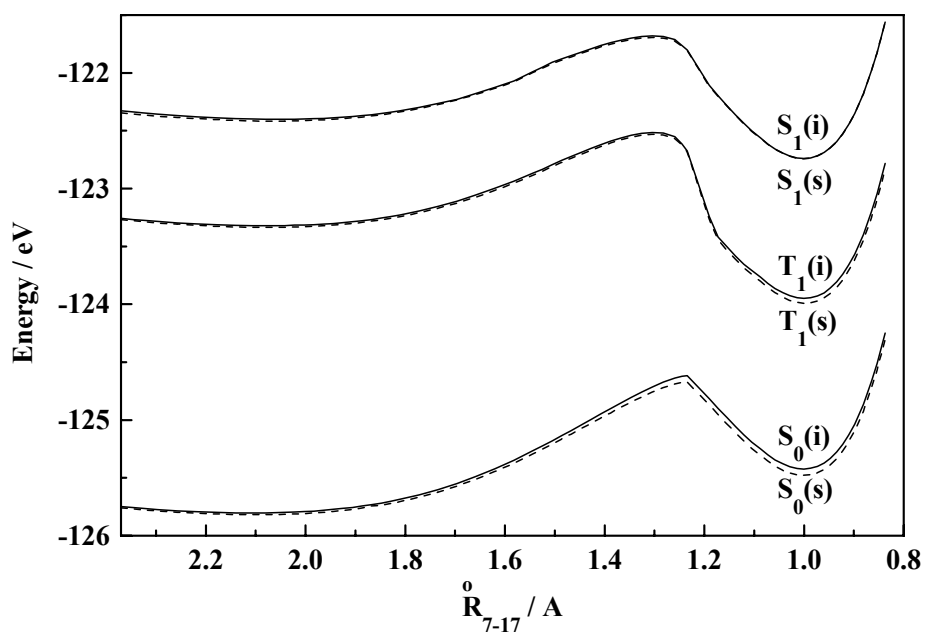
Figure 9. Simulated PECs for IPT process of HBT in S_0, S_1 and T_1 states (i, isolated; s, solvated in ethanol).
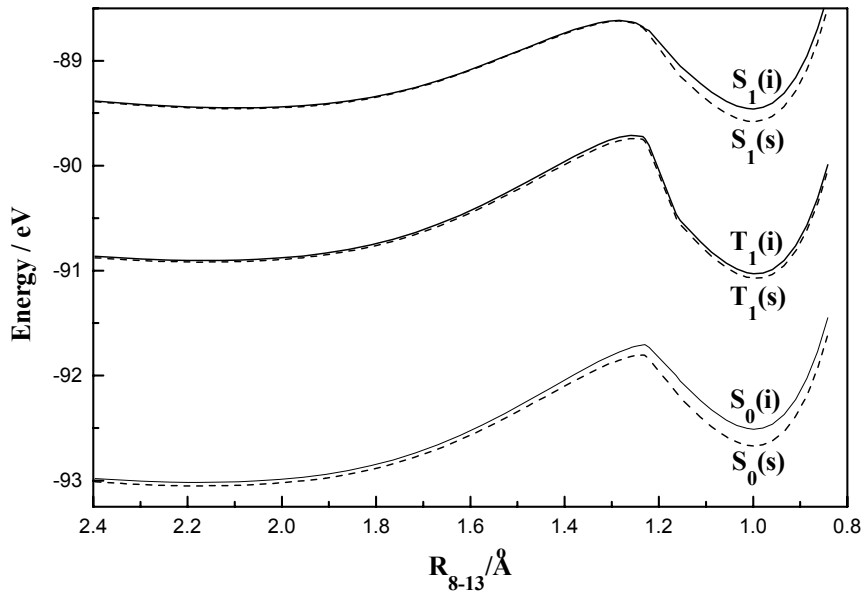

Figure 10. Simulated PECs for IPT process of HPO in S_0, S_1 and T_1 states (i, isolated; s, solvated in ethanol).
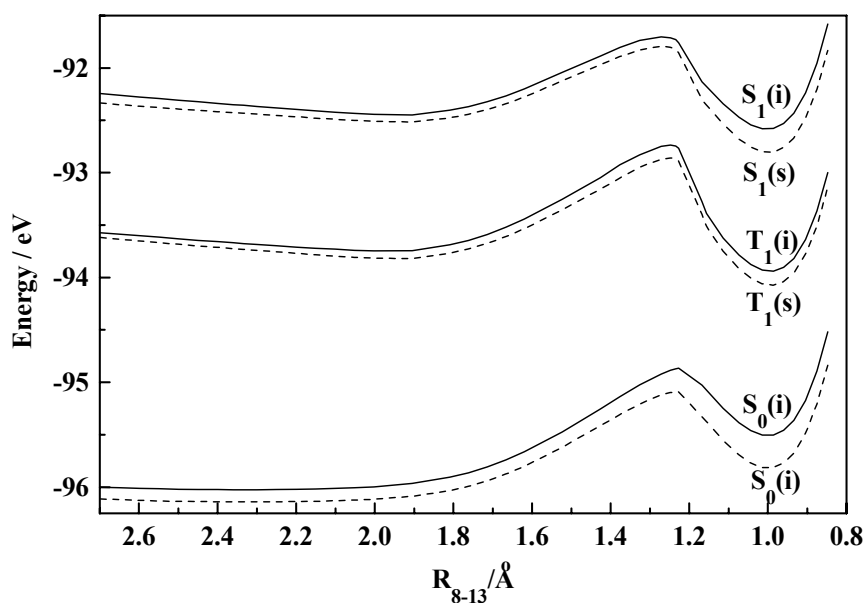
Figure 11. Simulated PECs for IPT process of HPI in S_0, S_1 and T_1 states (i, isolated; s, solvated in ethanol).
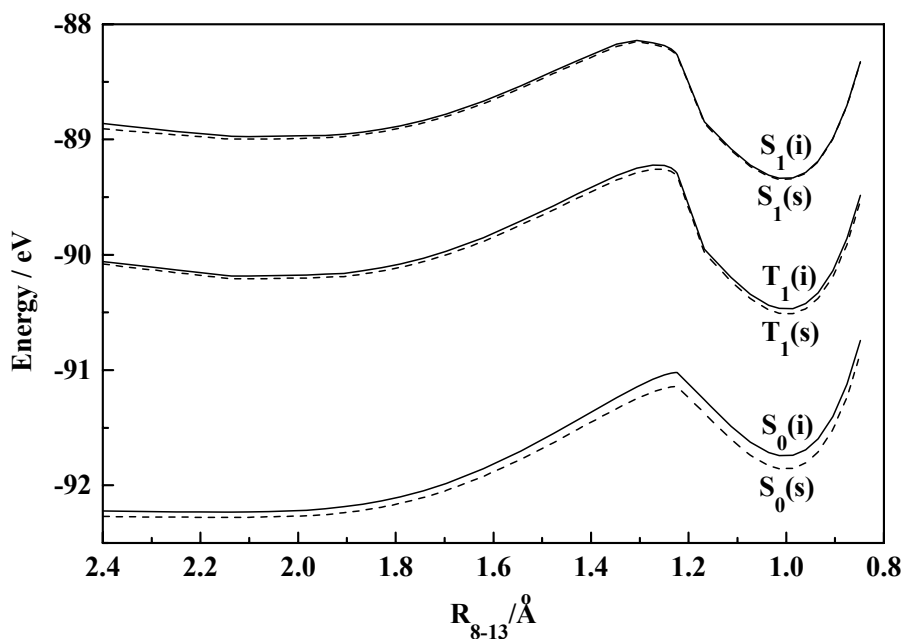

Figure 12. Simulated PECs for IPT process of HPT in S_0, S_1 and T_1 states (i, isolated; s, solvated in ethanol).

The figures clearly reveal that for all the fluorophores the formation of the tautomer via intramolecular proton transfer (IPT) in the ground state leads to endothermicity. However, the reaction becomes exothermic in S_1 as well as in T_1 states. This points to an unfavourable situation for the process in the ground state and a thermodynamic favour for the reaction in the lowest excited singlet

and triplet states. Considering the kinetic aspect for the process, the present calculations reveal that the activation barrier for the process is quite high for all the molecular systems in the ground state leading to impose a restriction on the process. A considerable lowering of the activation barrier in the lowest excited singlet and triplet electronic states indicates that the IPT process is favoured in the excited states compared to the ground state. Tables 15 and 16 present the calculated kinetic (E_{act}) and thermodynamic (ΔH) parameters for the IPT process in different electronic states of the molecular systems of the two series.

Calculations on all the molecular systems, thus, indicate that the activation barrier for the IPT reaction in the ground state is appreciably higher than those obtained in the lowest excited singlet (S_1) and triplet (T_1) states. As has been discussed before, the ΔH parameter also favours the proton transfer reaction in the excited states compared to the S_0 state. Hence, although the IPT process in infeasible in the ground state, the photoinduced proton transfer reaction is feasible in the S_1 and the T_1 states from both thermodynamic and kinetic reasons. The activation barriers from our calculations appear to be a little higher than the experimental values [11,16,25,27,37,48,53]. This deviation may be because of the fact that the short range specific interactions, like hydrogen bonding, have not been considered in the present work. In any case, for all the systems the predicted trends of the occurrence of the photoprocesses and the spectral patterns match well with the experimental results.

Table 15. Calculated activation energies (E_{act} in eV) and reaction enthalpies (ΔH in eV) for the intramolecular proton transfer reaction of HBO, HBI and HBT in S_0, S_1 and T_1 states.

Medium / Solvent	State	HBO		HBI		HBT	
		$E_{act.}$	ΔH	$E_{act.}$	ΔH	$E_{act.}$	ΔH
vacuum	S_0	1.251	+ 0.394	1.075	+ 0.335	1.187	+ 0.380
	S_1	0.892	- 0.088	0.781	- 0.236	0.722	- 0.338
	T_1	0.975	- 0.375	0.829	- 0.448	0.806	- 0.627
cyclohexane	S_0	1.239	+ 0.371	1.050	+ 0.306	1.170	+ 0.362
	S_1	0.892	- 0.102	0.777	- 0.250	0.722	- 0.333
	T_1	0.972	- 0.385	0.820	- 0.460	0.806	- 0.639
p-dioxane	S_0	1.238	+ 0.369	1.047	+ 0.302	1.168	+ 0.361
	S_1	0.892	- 0.103	0.777	- 0.252	0.722	- 0.332
	T_1	0.972	- 0.386	0.819	- 0.462	0.806	- 0.641
ethanol	S_0	1.223	+ 0.340	1.015	+ 0.266	1.146	+ 0.339
	S_1	0.893	- 0.121	0.772	- 0.269	0.723	- 0.326
	T_1	0.968	- 0.399	0.807	- 0.477	0.805	- 0.656
acetonitrile	S_0	1.223	+ 0.339	1.014	+ 0.265	1.145	+ 0.338
	S_1	0.893	- 0.121	0.772	- 0.270	0.723	- 0.325
	T_1	0.968	- 0.400	0.807	- 0.477	0.805	- 0.656
water	S_0	1.222	+ 0.338	1.013	+ 0.263	1.144	+ 0.337
	S_1	0.893	- 0.122	0.772	- 0.270	0.723	- 0.325
	T_1	0.967	- 0.400	0.807	- 0.478	0.805	- 0.657

Table 16. Calculated activation energies (E_{act} in eV) and reaction enthalpies (ΔH in eV) for the intramolecular proton transfer reaction of HPO, HPI and HPT in S_0, S_1 and T_1 states.

Medium / Solvent	State	HPO		HPI		HPT	
		$E_{act.}$	ΔH	$E_{act.}$	ΔH	$E_{act.}$	ΔH
vacuum	S_0	1.311	+ 0.508	1.159	+ 0.523	1.212	+ 0.491
	S_1	0.834	- 0.010	0.744	- 0.132	0.834	- 0.361
	T_1	1.193	- 0.126	1.009	- 0.193	0.962	- 0.284
cyclohexane	S_0	1.283	+ 0.453	1.113	+ 0.440	1.179	+ 0.462
	S_1	0.835	- 0.058	0.735	- 0.197	0.839	- 0.356
	T_1	1.186	- 0.138	0.987	- 0.221	0.957	- 0.292
p-dioxane	S_0	1.279	+ 0.447	1.108	+ 0.431	1.175	+ 0.459
	S_1	0.835	- 0.063	0.733	- 0.204	0.840	- 0.355
	T_1	1.185	- 0.140	0.985	- 0.224	0.956	- 0.293
ethanol	S_0	1.244	+ 0.380	1.051	+ 0.329	1.135	+ 0.423
	S_1	0.835	- 0.122	0.722	- 0.287	0.846	- 0.348
	T_1	1.177	- 0.155	0.957	- 0.257	0.950	- 0.303
acetonitrile	S_0	1.242	+ 0.377	1.048	+ 0.324	1.133	+ 0.421
	S_1	0.835	- 0.125	0.722	- 0.287	0.846	- 0.348
	T_1	1.177	- 0.156	0.956	- 0.259	0.950	- 0.303
water	S_0	1.241	+ 0.374	1.046	+ 0.320	1.131	+ 0.420
	S_1	0.835	- 0.127	0.716	- 0.295	0.847	- 0.347
	T_1	1.177	-0.156	0.955	-0.260	0.950	-0.304

Conclusion

The present work develops a comprehensive picture about the rotamerization and the intramolecular proton transfer processes of the two series of compounds in different electronic states. An effort has been made to sum up the photophysical behaviour of the compounds in some common homogeneous solvents. The calculated excitation, fluorescence and phosphorescence spectra agree well with the available experimental results concerning the photophysical phenomena. The above results and related discussion lead to the following relevant points regarding the fluorophores:

HBO and HBI have two rotameric forms (I and II) in the ground state while HBT exists only in the normal form (I) under similar condition. This corroborates the observation of three fluorescence bands from HBO and HBI and only a dual emission from HBT.

So far as the other series of compounds is concerned, in vacuum and in the common solvents, HPO gives rise to two rotameric forms in the ground state through a rotation about the single bond connecting the phenol ring and the azole ring. On the other hand, no stability to the rotamer (II) is offered by HPT leading only to the existence of the normal form (I) in all such conditions. For HPI, both the normal (I) and the rotamer (II) can be obtained in isolated condition or in solvents of low polarity while in high polarity solvents only the normal form survives.

Compounds of both the series consolidate that the intramolecular proton transfer (IPT) reaction is unfavourable in the ground state from both the thermodynamic as well as kinetic reasons. However, both the factors favour the excited state intramolecular proton transfer (ESIPT) process in the lowest excited singlet and triplet states.

Acknowledgements

References

1. Strandjord, A.J.G., Courtney, S.H.D., Friedrich, M., Barbara, P.F. *J. Phys. Chem.* **1983**, *87*, 1125.
2. Formosinho, S.J., Arnaut, L.G. *J. Photochem. Photobiol. A* **1993**, *75*, 21.
3. Flom, S.R., Barbara, P. F. *Chem. Phys. Lett.* **1983**, *94*, 488.
4. Chudoba, C., Riedle, E., Pfeiffer, M., Elsaesser, T. *Chem. Phys. Lett.* **1996**, *263*, 622.
5. Rodriguez, M.C.R., Rodriguez-Prieto F., Mosquera, M. *Phys. Chem. Chem. Phys.* **1999**, *1*, 253.
6. Brauer, M., Mosquera, M., Perez-Lustres, J. L., Rodriguez-Prieto, F. *J. Phys. Chem.* **1998**, *102*, 10736.
7. Roberts, E. L., Dey, J., Warner, I. M. *J. Phys. Chem.* **1996**, *100*, 19681.
8. Eisenberger, H., Nickel, B., Ruth, A.A., Al-Soufi W., Grellmann, K. H. *J. Phys. Chem.* **1991**, *95*, 10509.
9. Kundu, S., Bera, S. C., Chattopadhyay, N. *Ind. J. Chem. A* **1995**, *34*, 55.
10. Wiechmann, M., Port, H., Frey, W., Larmer F., Elsaesser, T. *J. Phys. Chem.* **1991**, *95*, 1918.
11. Sinha, H.K., Dogra, S. K. *Chem. Phys.* **1986**, *102*, 337.
12. O'Connor, D.B., Scott, G.W., Coulter, D.R., Yavroulan, A. *J. Phys. Chem.* **1991**, *95*, 10252.
13. Chou, P.T., Martinez, M.L., El-Sayed, M.A. *J. Phys. Chem.* **1993**, *97*, 2618.
14. Lin, G.C., Awad, E.S., El-Sayed, M.A. *J. Phys. Chem.* **1991**, *95*, 10442.
15. Caldin, E.F., Gold, V. *Proton Transfer Reactions,* Chapman and Hall: London, 1975.
16. Das, K., Sarkar, N., Ghosh, A.K., Majumdar, D., Nath, D.N., Bhattacharyya, K. *J. Phys. Chem.* **1994**, *98*, 9126.
17. Schwartz, B.J., Peteanu, L.A., Harris, C.B. *J. Phys. Chem.* **1992**, *96*, 3591.
18. Ernsting, N.P., Arthen-Engeland, Th., Rodriguez, M.A., Thiel, W. *J. Chem. Phys.* **1993**, *97*, 3914.
19. Frey, W., Elsaesser, T. *Chem. Phys. Lett.* **1992**, *189*, 565.
20. Wiechmann, M., Port, H., Frey, W., Lärmer, F., Elsaesser, T. *Chem. Phys. Lett.* **1990**, *165*, 28.
21. Lärmer, F., Elsaesser T., Kaiser, W. *Chem. Phys. Lett.* **1988**, *148*, 119.
22. Rios, M.A., Rios, M.C. *J. Phys. Chem.* **1995**, *99*, 12456.
23. Douhal, A., Lahmani, F., Zehnacker-Rentien, A., Amat-Guerri, F. *J. Phys. Chem.* **1994**, *98*, 12198.

24. Bräuer, M., Mosquera, M., Pérez-Lustres, J.L., Rodriguez-Prieto, F. *J. Phys. Chem. A* **1998**, *102*, 10736.

25. Guallar, V., Moreno, M., Lluch, J.M., Amat-Guerri, F., Douhal, A. *J. Phys. Chem.* **1996**, *100*, 19789.

26. Premvardhan, L., Peteanu, L. *Chem. Phys. Lett.* **1998**, *296*, 521.

27. LeGourriérec, D., Kharlanov, V.A., Brown, R.G., Rettig, W. *J. Photochem. Photobiol. A* **2000**, *130*, 101.

28. Potter, C.A.S., Brown, R.G., Vollmer, F., Rettig, W. *J. Chem. Soc. Faraday Trans. 1* **1994**, *90*, 59.

29. Rodriguez, M.C.R., Rodriguez-Prieto, F., Mosquera, M. *Phys. Chem. Chem. Phys.* **1999**, *1*, 253.

30. Santra, S., Krishnamoorthy, G, Dogra, S.K. *Chem. Phys. Lett.* **2000**, *327*, 230.

31. Cohen, M.D., Flavian, S.J. *J. Chem. Soc. B* **1967**, 317.

32. Cohen, M.D., Flavian, S.J. *J. Chem. Soc. B* **1967**, 321.

33. Elsaesser, T., Kaiser, W. *Chem. Phys. Lett.* **1986**, *128*, 231.

34. Elsaesser, T., Schmetzer, B., Lipp, M., Bäuerle, R.J. *Chem. Phys. Lett.* **1988**, *148*, 112.

35. Al-Soufi, W., Grellmann, K.H., Nickel, B. *J. Phys. Chem.* **1991**, *95*, 10503.

36. Douhal, A., Kim, S.K., Zewail, A.H. *Nature* **1995**, *378*, 260.

37. Das, K., Sarkar, N., Majumdar D., Bhattacharyya, K. *Chem. Phys. Lett.* **1992**, *198*, 443.

38. Mishra, A.K., Dogra, S.K.; *Ind. J. Phys. B*, **1984**, *58*, 480.

39. Woolf, G.J., Melzig, M., Schneider, S., Dörr, F. *Chem. Phys.* **1983**, *77*, 213.

40. Mordzinski, A., Grellmann, K.H. *J. Phys. Chem.* **1986**, *90*, 5503.

41. Potter, C.A.S., Brown, R.G. *Chem. Phys. Lett.* **1988**, *153*, 7.

42. Ding, K., Courtney, S.J., Strandjord, A.J., Flom, S., Friedrich, D., Barbara, P.F. *J. Phys. Chem.* **1983**, *87*, 1184.

43. Nakagaki, R., Kobayashi, T., Nagakura, S. *Bull. Chem. Soc. Jpn.* **1978**, *51*, 1671.

44. Nagaoka, S., Kusunoki, J., Fujibuchi, T., Mukai, K., Nagashima, U. *J. Photochem. Photobiol. A* **1999**, *122*, 151..

45. Nagaoka, S., Itoh, A., Mukai, K., Nagashima, U. *J. Phys. Chem.* **1993**, *97*, 11385

46. Williams, D.L., Heller, A. *J. Phys. Chem.* **1970**, *74*, 4473.

47. Becker, R.S., Lenoble, C., Zein, A. *J. Phys. Chem.* **1987**, *91*, 3509.

48. Arthen-Engeland, Th., Bultmann, T., Earnsting, N.P., Rodriguez, M.A., Thiel, W. *Chem. Phys.* **1992**, *163*, 43.

49. Lavtchieva, L., Enchev, V., Smedarchina, Z. *J. Phys. Chem.* **1993**, *97*, 306.

50. Forés, M., Duran, M., Solà, M., Adamowicz, L. *J. Phys. Chem. A* **1999**, *103*, 4413.

51. Purkayastha, P., Chattopadhyay, N. *Phys. Chem. Chem. Phys.* **2000**, *2*, 203.

52. Purkayastha, P., Chattopadhyay, N. *J. Mol. Struct.* **2002**, *604*, 87.

53. Catalan, J., Fabero, F., Guijarro, M.S., Claramunt, R.M., Santa Maria, M.D., Foces-Foces, M. de la Concepcion, Cano, F.H., Elguero, J., Sastre, R *J. Am. Chem. Soc.* **1990**, *112*, 747.

54. Dick, B. *J. Phys. Chem.* **1990**, *94*, 5752.

55. Purkayastha, P., Bhattacharyya, P.K., Bera, S.C., Chattopadhyay, N. *Phys. Chem. Chem. Phys.* **1999**, *1*, 3253.

56. HYPERCHEM 5.01, Hypercube Inc., Canada.

57. Bottcher, C.J.F. *Theory of Electronic Polarization,* Vol. I., Elsevier: Amsterdam, 1983.

58. Stenson, P. *Acta Chem. Scand*. **1970**, *24*, 3729.

59. Elerman, Y., Kabak, M. *Acta Cryst. C* **1997**, *53*, 372.

60. Purkayastha, P. *Ph.D. Dissertation*, Jadavpur University, **2002.**

61. Cramer, C.J., Truhlar, D.G. *Quantitative Treatment of Solute/Solvent Interactions*; Politzer, P.; Murray, J.S., Eds.; Vol. I, Elsevier: Amsterdam, 1994.

62. Nandi, N., Bhattacharyya, K., Bagchi, B. *Chem. Rev.* **2000**, *100*, 2013.

63. Ingham, K.C., El-Bayoumi, M.A. *J. Am. Chem. Soc*. **1974**, *96*, 1682.